Lawrence Berkeley National Laboratory

Title
CHARACTERISTICS OF NEUTRAL MESON PRODUCTION IN THE PROTON BOMBARDMENT OF CARBON NUCLEI

Permalink
https://escholarship.org/uc/item/4zh9c49n

Authors
Crandall, Walter E.
Moyer, Burton J.

Publication Date
1953-02-13

UNIVERSITY OF CALIFORNIA – BERKELEY

RADIATION LABORATORY

DISCLAIMER

UNIVERSITY OF CALIFORNIA

Radiation Laboratory

Contract No. W-7405-eng-48

CHARACTERISTICS OF NEUTRAL MESON PRODUCTION IN THE PROTON BOMBARDMENT OF CARBON NUCLEI

Walter E. Crandall and Burton J. Moyer

February 13, 1953

Berkeley, California

CHARACTERISTICS OF NEUTRAL MESON PRODUCTION IN THE PROTON BOMBARDMENT OF CARBON NUCLEI

Walter E. Crandall and Burton J. Moyer

Department of Physics and Radiation Laboratory
University of California, Berkeley, California

February 13, 1953

I. INTRODUCTION

During the period since the first article[1] identifying the photon radiation ascribed to π^o meson decay in the cyclotron target, the development of improved pair spectrometer equipment and techniques has allowed a better and more complete measurement of the photon spectrum than was there presented.

Out of these more detailed spectrum data information may be derived concerning the energy distribution of the emission of π^o mesons from a target bombarded by high-energy protons, and of the angular distribution with which they emerge from proton-nucleon collisions. Also an evaluation of the absolute yield has been made for the case of 340 Mev protons incident upon carbon nuclei and the variation of yield with proton energy determined. These allow comparison with the recent work of Marshall, et al[2] at the Chicago cyclotron.

The basic physical measurements consisted of determinations of the photon spectra radiated from the cyclotron target in various directions with respect to the incident proton beam. These were all monitored in relative intensity, and finally the spectrum in the 90° direction was placed upon an absolute scale by calculation of the pair spectrometer spectral efficiency and measurement of the proton beam current.

Deductions concerning angular and energy distributions are possible in view of the assumed unique origin of the photons: $\pi^o \longrightarrow 2\gamma$. The degree to which other processes may contribute to the high-energy photon yield is not definitely known, but certain symmetry tests upon the experimental spectra indicate that such contributions may be very small relative to the π^o photon yield.[3,4]

II. SPECTRAL PROPERTIES OF THE π^o DECAY RADIATION

A. The Total Spectrum: Its Symmetry

Calculation of an expected gamma ray spectrum for a given angular direction with respect to the incident proton beam would require prior knowledge of the angular and energy distributions with which the π^o mesons are created. The properties of the total spectrum, however, are independent of angular distribution and may be put to experimental test. By "total spectrum" we mean the composite spectral emission obtained by integrating over all solid angular space surrounding the target.

It is this total spectrum with which the work of the Bristol group[5] deals in their photographic emulsion study of photons accompanying cosmic ray star events. Professor W. K. H. Panofsky recognized the possibility of constructing a total spectrum from measurements which could be made at the Berkeley cyclotron and of deducing from it the energy distribution of the π^o's together with a possible indication of non-π^o high-energy photon emission. The pertinent features of the total spectrum are developed in reference 5, and will now be briefly presented here in a somewhat different manner more closely related to the experiment.

Consider a π^o meson moving relative to the laboratory with velocity $c\beta$ indicated in Fig. 1. It decays into two photons which, in the π^o rest frame, have equal energy, k_o, and opposite directions. Due to aberration, the photon emitted at angle α in the π^o rest frame is received in the laboratory at angle ϕ with respect to the π^o motion and with energy k, where (with $\gamma = (1 - \beta^2)^{-1/2}$)

$$k = k_o \gamma (1 + \beta \cos \alpha) \tag{1}$$

and,
$$\cos \phi = \frac{\cos \alpha + \beta}{1 + \beta \cos \alpha} \tag{2}$$

Thus, for a given β, energy increments in the observed laboratory spectrum depend simply upon increments in the emission angle α according to

$$d k = - k_o \gamma \beta \sin \alpha \, d \alpha \tag{3}$$

Now in the total spectrum all values of α contribute with equal probability. So out of a large number of π^o decay events, the number $d n_\beta$ of photons, arising from mesons of velocity $c\beta$, within $d\alpha$ at angle α is (with two photons per π^o)

$$d\, n_\beta = N(\beta) \sin \alpha\, d\, \alpha \tag{4}$$

where $N(\beta)$ is the number of π^o's per unit range in β at velocity $c\beta$.

Thus in the total spectrum arising from decay of π^o mesons of this velocity the spectral intensity is, in view of (3) and (4)

$$\left| \frac{d\, n}{d\, k} \right|_\beta = \frac{N(\beta)}{k_o \beta \gamma} = \text{const.} \tag{5a}$$

between the limits (given by use of (1)) of

$$k_1(\beta) = k_o \sqrt{\frac{1-\beta}{1+\beta}}\,, \text{ and } k_2(\beta) = k_o \sqrt{\frac{1+\beta}{1-\beta}} \tag{5b}$$

It is clear then that the total spectrum contributed by π^o's with various values of β is compounded out of differential rectangular increments as qualitatively suggested in Fig. 2, and that the spectral intensity $I(k)$ is given by integrating (5a) to obtain

$$I(k) = \int_{\beta'(k)}^{\beta_{max}} \frac{N(\beta)}{k_o \beta \gamma}\, d\beta \tag{6a}$$

where $\beta'(k)$ is the smallest relative velocity which can yield a laboratory photon energy of k, namely, by (5b)

$$\begin{cases} \beta'(k) = \dfrac{k^2 - k_o^2}{k^2 + k_o^2}\,, \text{ for } k > k_o \\[2mm] \beta'(k) = \dfrac{k_o^2 - k^2}{k_o^2 + k^2}\,, \text{ for } k < k_o \end{cases} \tag{6b}$$

In view of Eqs. (5b), and from the construction of Fig. 2, the symmetry property of the total spectrum is evidently of the type $k_1 k_2 = k_o^2$. If the abscissa scale is made logarithmic the spectrum curve should show simple symmetry with respect to a vertical line at $\log k_o$. This is to be applied as a test to the experimental data to indicate possible presence of non-π^o photon radiation.

B. Deduction of Meson Energy Distribution

The velocity distribution function $N(\beta)$ may be evaluated at the lower limit β' by differentiation of Eq. (6a) and use of numerical data from the experimental total spectrum. Thus

$$N(\beta') = \beta' \gamma'^3 k_o\, k \frac{dI}{dk}$$

where the associated values of β' and k are obtained from (6b).

This is readily transformed into a total-energy distribution function, since $E' = 2 \gamma' k_0$. The result is

$$N(E') = \frac{k}{2} \left| \frac{dI}{dk} \right|$$

where $E' = \frac{k^2 + k_0^2}{k}$ (7)

The best experimental spectrum data exist in the region $k \geq k_0$, so only the high-energy side of the spectrum peak will actually be used in obtaining values of $\left| \frac{dI}{dk} \right|$. E' is total energy, i.e., $M_{\pi 0} C^2 + KE$, or $2k_0 + KE$.

All the foregoing characteristics derived for the total spectrum would apply also to a π^0 photon spectrum observed within any reference frame in which the π^0 angular distribution were spherically symmetric, if such a reference frame existed.

C. Information on Angular Distribution of π^0 Meson Emission

In Fig. 3 is depicted the basis upon which some angular distribution information may be deduced. Let the spectrum observed in a direction θ be $I(\theta, k)$. All photons received of energy above an assigned lower limit k_1 will arise solely from π^0 mesons of energy greater than $E_1 = \frac{k_1^2 + k_0^2}{k_1}$ emitted within a cone of solid angle opening about the direction of the observer; and the angular width γ_{max} of the cone is determined by the maximum total energy, E_{max}, with which the mesons may be created according to the relation

$$\cos \gamma_{max} = \frac{E_{max} - 2 \frac{k_0^2}{k_1}}{\sqrt{E_{max}^2 - 4k_0^2}}$$ (8)

By choosing k_1 sufficiently large, the size of the cone may be made arbitrarily small, and it becomes reasonable to treat the contribution of mesons emitted within the cone as if it were a small sample of a spherically symmetric emission. Use of relationship (7) then permits deduction of the energy distribution $N(E, \theta)$, for the high-energy tail of the mesons emitted in the direction θ. If the proper value of E_{max} to be associated with θ were everywhere known, it would now be possible to develop the angular distribution of mesons of various energies in the region of the high-energy tail.

The basic reference frame in which the π^0 production occurs is the center-of-mass system for an incident beam proton and the target nucleon which

forms its collision partner. The angular distribution of π^o emission in this system is desired, and the value of E_{max} within this system is presumably independent of angle. However, due to the motion of nucleons within nuclei there is no unique CM system, but rather a distribution of CM velocities about a mean value; but if the incident proton momentum is large compared to nucleon momenta in the target this spread of CM velocities is relatively small.

Determination of a mean CM velocity is possible by analyzing the Doppler shift of the photon spectra seen in observations at 0° and 180° with respect to the proton beam under the assumption of similar spectral emission at these angles in the CM system. The various spectra observed at different laboratory angles-of-view may then be transformed into related spectra in the mean CM system by the relations

$$I_c(k_c, \theta_c) = \gamma(1 - \beta \cos \theta) I (k, \theta)$$

$$k_c = k \gamma (1 - \beta \cos \theta)$$

$$\cos \theta_c = \frac{\cos \theta - \beta}{1 - \beta \cos \theta}$$

$$(9)$$

where the "c" subscripts denote quantities in this CM system, and the quantities β and γ refer to the motion of the center-of-mass with respect to the laboratory.

The analysis described in the foregoing paragraphs of this section then allows features of the angular distributions of the high-energy mesons in this mean CM system to be inferred.

III. THE EXPERIMENTAL SPECTRA

A. Cyclotron Facilities

Cyclotron tank windows, target-support probes, and holes through the concrete shielding limited the angles-of-view for the pair spectrometer to 0°, 47°, 90°, 133°, and 180°. These are angles of photon emission measured from the direction of the proton beam as it strikes the target placed at a radius of 80-1/2 in. in the cyclotron tank.

The pair spectrometer was in all cases outside the cyclotron shielding, at a typical distance of 60 ft. from the target.

For the absolute yield determination described in Section VI, the external, deflected proton beam was employed; but its intensity is too low for good spectrum data.

B. Pair Spectrometer

The pair magnet was originally designed by Professor H. F. York and Mr. Paul Hernandez for this type of spectroscopy. The system of geiger and proportional counters employed is that developed by Panofsky, Aamodt, and Hadley[6] for their work on the capture of π^- mesons in hydrogen and deuterium. In Fig. 4 are portrayed the magnet, converter, and counter system.

An electron pair triggers each of the two-chambered proportional counters. This quadruple coincidence initiates a 1-1/2 microsecond gate which is fed to the geiger tube amplifiers, allowing them to register any events occurring during the gate duration. If the background counting rate is within limits, only the two geiger tubes traversed by the pair particles will show signals within the gate period, and these define the two electron orbit radii and hence the photon energy.

Recording of the geiger coincidence pairs in proper energy channels was accomplished by use of a 14-element square matrix array consisting of 196 coincidence units. The coincidence outputs were grouped into 27 energy channels which were registered. The development of this matrix system was promoted by Dr. Darcy Walker,[3,4] and is in principle an elaboration of the original system of this type used by MacDaniel, et al.[7]

The various corrections which must be applied to the raw spectrometer data involve energy channel efficiencies, variations in pair production cross section, scattering loss calculations, electron energy loss in the converter, et cetera. These are discussed in the appendix.

The total energy span of the spectrometer does not include the complete spectrum for a given magnetic field setting, so that typically three separate settings were involved in a single spectrum determination. The agreement of extensive overlap regions gave confidence as to the validity of the data and its treatment.

C. Experimental Spectrum Results at 340 Mev

Displayed in Fig. 5 are the spectra obtained at various angles-of-view in the laboratory. The ordinate is plotted on an absolute scale as the cross section presented by a carbon nucleus for the production of a photon of energy k into unit solid angle in direction θ. The means of establishing an absolute scale will be discussed in Section VI.

Monitoring of the separate runs to provide proper relative intensity values was accomplished by use of thin aluminum foils mounted on the target.

Generation of Na^{24} activity by the reaction: Al^{27}(p; 3p, n)Na^{24} gave relative integrated proton flux values. Excitation of C^{11} in polystyrene foils on the target has also been employed for monitoring in some cases; the bombardment time then being less than the C^{11} half-life.

IV. THE TOTAL SPECTRUM, AND DEDUCTIONS FROM IT

A. Method of Construction

In order to compose the spectra observed into a total emission spectrum it is necessary to associate with each experimental spectrum a solid angle weighting factor. Thus it was assumed that the spectrum observed at $0°$ was representative of the photon emission in the forward cone out to $30°$; the spectrum at $47°$ was taken as representative of the emission in the conical interval from $30°$ to $60°$; the 90° spectrum served for the interval $60° - 120°$; the $133°$ spectrum for $120° - 150°$; and the $180°$ spectrum for the backward cone, $150° - 180°$. Each of the spectra of Fig. 5 were multiplied by the solid angle contained within the associated interval and these products added to obtain the total spectrum of Fig. 6. A logarithmic abscissa scale is used to facilitate the test for symmetry. Within reasonable limits, variation in the choice of angular intervals does not affect the form of the total spectrum enough to modify the conclusions drawn from it in the ensuing discussion.

B. Comments on Symmetry

In Section II - A, it was shown that a symmetry of the type $k_1 k_2 = k_0^2$ will obtain if all photons arise from $\pi°$ decay, where k_1 and k_2 are minimum and maximum energies for a given intensity, respectively, and k_0 is the proper energy of a $\pi°$ decay photon.

The present experimental data for photon energies below the peak are so poor as to make the symmetry test of questionable significance. The four dotted curves on the low-energy side of Fig. 6 correspond to reflections of the spectrum at vertical lines with the energies indicated. Clearly no definite conclusion may be drawn until better low-energy data from a modified spectrometer under preparation are available.

If, however, one demands a value of k_0 given by the experiments of Panofsky, et al,[6] namely 67.5 Mev, the symmetry criterion does not appear to be well satisfied. It would be necessary to conclude that some radiation in addition to $\pi°$ photons contributes particularly in the region above k_0. The total

amount of photon emission to be subtracted away from the spectrum in order to produce symmetry need be only about 5 percent of the total emission,[4] though this might possibly represent of course only a minimum value.

Possible origins of non-π^o photon emission are provided by such processes as:

(1) Radiative capture by neutrons of protons in flight (inverse photo-disintegration of deuteron).

(2) Radiative capture of mesons in flight within the same nucleus in which they are produced.

(3) Bremsstrahlung from proton-nucleon collisions. These can give rise to photons in the required energy region, but the yield of photons from them is theoretically estimated to be not more than a few percent of the π^o yield, and the spectrum from process (3) would be heavily weighted toward low photon energies, and would not be expected to contribute selectively in the energy region involved here to account for non-symmetry.

In view of the poor spectrum data below the k_o energy it is not possible to claim that the observation of non-π^o photons has been certainly demonstrated; and since the yield from other processes is expected to be relatively very small, the total spectrum will tentatively be considered to arise solely from π^o decay in the further topics of the present paper. Further justification for this is presented in Section VI - C.

C. Energy Distribution of π^o Mesons

By carrying out the operations indicated in Section II - B, using Eqs. (7), the distribution in total π^o energy in the laboratory reference frame is deduced. Only the high-energy side of the total spectrum is used in obtaining the values of $\frac{dI}{dk}$. The result, when converted into a distribution in kinetic energy of emission is displayed in Fig. 7.

Cladis, Hess, and Moyer,[8] and Wolf[9] have experimentally obtained a momentum distribution for nucleons in a carbon nucleus. By use of their results, it is possible to calculate the distribution in energy available in the collisions of 340 Mev protons with nucleons of the carbon nucleus. When this distribution in available energy is multiplied by an energy dependence for π^o production in proton-nucleon collisions, the resulting energy distribution of the mesons when transformed into the laboratory frame is compatible with that observed in Fig. 7, when certain plausible assumptions are made about the excitation energy of the residual nuclear system.

The calculations of Henley and Huddlestone[10] on the production of π^- mesons in the proton bombardment of carbon employed a nucleon momentum distribution similar to that of reference 8. They obtained satisfactory agreement with available experimental data on π^- energy distributions, which were very much like Fig. 7.

V. ON THE ANGULAR DISTRIBUTION OF π^0 EMISSION

A. Mean Center of Mass Velocity

In Section II - C the means of inferring a mean velocity of the CM system for the nucleon collisions producing π^0 mesons was defined. Actually the simplest practical means of evaluating β, assuming forward-backward symmetry in the CM frame, is provided by observing that from relations (9) may be deduced the following relations between the 0° and 180° spectra, involving the relative velocity β of the CM

$$I(k, \ 0^\circ) = \frac{1 + \beta}{1 - \beta} \ I(k', \ 180^\circ)$$

$$k = \frac{1 + \beta}{1 - \beta} \ k' \tag{10}$$

Thus, intensity and energy both transform by the same multiplicative factor, so that on a log-log plot the 0° and 180° spectra should coincide upon sliding one spectrum in a forty-five degree direction until it best overlaps the other. The amount of translation along either axis will evaluate $\frac{1 + \beta}{1 - \beta}$, and hence β. The shapes of the 0° and 180° spectra are experimentally better determined than the relative ordinates; so in evaluating β we have paid more attention to obtaining proper transformation of spectrum shape and energy values than to agreement of intensities. The latter do not quite coincide using $\beta = 0.3$, but seem to indicate somewhat greater emission at 0° than at 180° in the $\beta = 0.3$ frame.

Clearly this β is less than that for the CM frame of a 340 Mev proton and a stationary nucleon. The strong energy dependence of the π^0 production accentuates the contribution from collisions with nucleons moving counter to the proton. In fact the 0.3 value implies that the representative collision involves a nucleon in a carbon nucleus moving toward the proton with a velocity of 0.218c or a kinetic energy of 23 Mev.

B.   Deduction of Angular Distributions in CM System

By use of relations (9) the spectra in the five laboratory directions, $0°$, $47°$, $90°$, $133°$, and $180°$ are now transformed into the related spectra in the mean CM system at the respective related angles, $0°$, $59°$, $108°$, $146°$, and $180°$.   As described in Section II - C, the high energy tails of these CM spectra are now to be differentiated for use in Eqs. (7) to yield energy distributions for the neutral mesons emitted in the angular direction involved, within a cone whose generating angle is given by Eq. (8) for chosen values of E_{max} and k_1.

The collision of a 340 Mev proton with a nucleon in a carbon nucleus so moving as to provide a CM frame whose projected motion along the proton beam direction has a relative velocity $\beta = 0.3$ provides, by calculation, a maximum available energy* of $E_{max} = 215$ Mev, or a maximum $\pi°$ kinetic energy of about 80 Mev.   Due to the distribution of nucleon momenta, however, meson kinetic energies in this reference frame will extend from essentially zero up to about 120 Mev in the forward direction, and up to values even higher in the backward direction.   Yet the "representative collision" which gives rise to the mean value of $\beta = 0.3$ will predominate sufficiently for reasonable momentum distributions and meson excitation functions to allow the following rough analysis of angular distributions in the CM frame.

If the photon spectra for various angles of view in the CM frame are limited to energies above $k_1 = 150$ Mev, the photons will arise from neutral meson emission within cones with generating angles γ_{max} (by use of Eq. (8)) of about $25°$ opening about the respective angles of view, as shown in Fig. 3.   The chosen lower limit, $k_1 = 150$ Mev, requires that a $\pi°$ meson possess at least 47 Mev kinetic energy to contribute to the spectrum region observed.

Now by application of Eq. (7), the kinetic energy distributions in the various directions are deduced, under the approximation that within the limited emission cone the angular distribution is treated as a portion of a spherically symmetric yield.   These are displayed in Fig. 8.   In Fig. 9 are sketched the angular distributions for mesons of certain energies, inferred from the data of Fig. 8.   In view of the calculation mentioned in the second paragraph above, the mesons with kinetic energies near 80 Mev should most nearly display the angular distribution in the CM frame for a proton-nucleon collision.

---

* It is necessary to take account of the energy carried away by the residual nuclear system in making these calculations.   If this is not done, unreasonably high values of available energy are calculated from the high momentum components in the nucleon motion.

While these results are admittedly very crude, they do infer a promi-
nent $\cos^2\theta$ contribution. In view of the known small yield of π^o mesons from
p - p collisions,[11] it is possible that these results indicate the presence of the
process $p + n \longrightarrow \pi^o + d$ within the bombarded carbon nucleus, which is expected
to yield the mesons with a prominent $\cos^2\theta$ distribution. Recent experiments
by R. H. Hildebrand[12] at Chicago, on the production of π^o mesons in free n - p
collisions, show an angular distribution for the process n (p, d) π^o described
by $a + b \cos^2\theta$, where $b/a \simeq 5$.

VI. THE ABSOLUTE YIELD: DEPENDENCE UPON ENERGY

A. The Absolute Yield Experiment

Since absolute evaluation of the proton current at an internal cyclotron
target at these energies is uncertain, the foregoing data were placed upon an
absolute scale by observing the photon yield at one angle and one spectrum region
from a target in the external proton beam. The fact that the external beam is
10^{-4} to 10^{-5} of the internal beam precluded the taking of more data in this man-
ner.

In Fig. 10 the method of this absolute determination is shown. The
pair spectrometer is mounted at a point where, by rotation, it can receive either
the photons from an internal target or those from a target in the monitored ex-
ternal proton beam. Proper plateau conditions for the spectrometer counters
are obtained with good counting rates by receiving photons from the internal
target. The internal target is then removed, and the spectrometer rotated so
as to receive photons from the external target. Just preceding the pair spec-
trometer is a photon aperture definer and clearing field. The aperture permits
only the converter foil of the spectrometer to "see" the target, and the clear-
ing field removes electron pairs produced in air and at the aperture surfaces.
The deflected beam passes through a calibrated ionization chamber just before
striking the target.

B. Converter Efficiency Correction. Absolute Yield Result

Absolute calibration of the pair spectrometer involves a number of
corrections to be applied to the basic data. These are discussed briefly in the
Appendix. One of the most important of these is the converter efficiency cor-
rection which involves the following features.

For conversion of photons at depth x in a converter of thickness t, the yield of detectable electron pairs will depend upon attenuation of the photons as they progress through the thickness x of the converter material to the lamina dx in which conversion occurs, and then upon the survival of both pair particles against scattering and radiative collisions in the interval $t - x$, which would remove them from the trajectories which are received by the counters.

Use of well known physical data relating to such processes allows the calculation of an "effective" converter thickness, less than the actual thickness, which in the absence of such attenuation and particle loss would yield the observed number of pairs. (Conversely, instead of considering the effective converter thickness, one could correct the pair yield for a given thickness by similar calculations.)

In the data of Fig. 11 the spectrometer counting rate is plotted as a function of effective thickness of Ta converter foil. Data of two different runs are presented; the different intercepts at zero thickness infer differences in efficacy of aperture and clearing field adjustments in removing undesired pairs. The initial sharp rise is probably due to conversion in the foil support device, but the extended linear portions are considered to represent by their slopes the correct conversion yield per unit thickness of Ta. From this, and the known pair production cross section, the absolute efficiency of the spectrometer may be established.

Since now an absolute yield of photons in the 90° direction, within a known spectrum interval of the total emission in this direction, is known, it becomes possible to place upon an absolute basis the relatively measured spectra in all the directions. Then by employment of solid angle weighting factors, as in the construction of the total spectrum in Section IV - A, the absolute total yield of photons is obtained.

Together with the measured value of proton beam current incident upon the target this results in a cross section for production of high-energy photons per carbon nucleus of:

$$\sigma_{photon} = (3.4 \pm 0.8) \times 10^{-27} \text{ cm}^2$$

Under the assumption that these are all from π° decay, the π° production cross section is:

$$\sigma_{\pi^\circ} = (1.7 \pm 0.4) \times 10^{-27} \text{ cm}^2,$$

per carbon nucleus for 340 Mev protons.

These values are not directly comparable with those of Marshall,[2] et al, at Chicago because of lack of precise knowledge of the energy dependence of the cross section. However, if the Z-dependence observed by Hales, et al,[11] is combined with an extension of the energy dependence presented below in Section VI - C, the present data predict a Be cross section at 430 Mev of $(5.8 \pm 1.5) \times 10^{-27} \text{ cm}^2$ which may be compared with $(8.7 \pm 2) \times 10^{-27} \text{ cm}^2$ observed by the Chicago group.

C. Variation of Yield with Proton Energy

Available shielding apertures permitted data to be obtained at reduced proton energies for certain supplementary pairs of angles-of-view. The spectra from these observations are displayed in Fig. 12.

These afford a further check on the smallness of radiation from sources other than π^0 decay. As the energy available for π^0 production approaches threshold, the incident protons must select nucleons moving with increasingly higher momenta opposite to their motion. Consequently the approach to a unique CM system is more evident in the smaller doppler shift of the spectra involved in changing the angle-of-view. Likewise, the decreasing available kinetic energy for the π^0 results in somewhat narrower peaks, since the peak breadth is due to the Doppler shift of photons from the moving mesons. Finally, any photons originating in radiative meson capture would be expected to produce more pronounced asymmetry of these spectra than of those at higher energies. Such does not appear to be the case.

By estimated reconstruction of the total photon emission upon the basis of the spectra observed at supplementary angles, it is possible to present the variation in π^0 production cross section as a function of incident proton energy. The result is given in Fig. 13. It is displayed together with a curve calculated by Brueckner for a pseudoscalar pion with pseudovector coupling and a typical momentum distribution[8] which has appeared to best fit other data in meson production.[10]

VII. ACKNOWLEDGEMENTS

square matrix coincidence circuit.   The fine cooperation of the cyclotron crew
under Messrs. James Vale and Lloyd Hauser has been much appreciated,

BIBLIOGRAPHY

1.   R. Bjorklund, W. Crandall, B. J. Moyer and H. F. York, Phys. Rev. 77, 213-18, (1950).

2.   J. Marshall, L. W. Marshall, V. A. Nedzel, and S. Warshaw, Phys. Rev. 88, 632-41, (1952).

3.   W. Crandall, K. M. Crowe, B. J. Moyer, W. K. H. Panofsky, R. H. Phillips, and D. Walker, Phys. Rev. 85, 771A (1952).

4.   W. Crandall, W. K. H. Panofsky, D. Walker, Private Communication.

5.   A. G. Carlson, J. E. Hooper, and D. T. King, Phil. Mag. 41, 701-24, (1950).

6.   W. K. H. Panofsky, R. L. Aamodt, and J. Hadley, Phys. Rev. 81, 565 (1951).

7.   B. D. MacDaniel, G. von Dardel, and R. L. Walker, Phys. Rev. 72, 985 (1947).

8.   J. B. Cladis, W. N. Hess, and B. J. Moyer, Phys. Rev. 87, 425-33 (1952).

9.   P. Wolf, Phys. Rev. 87, 434-8, (1952).

10.   E. M. Henley, Phys. Rev. 85, 204-15, (1952).

11.   R. W. Hales, and B. J. Moyer, Phys. Rev. 89, 1047-53, (1953).

12.   R. H. Hildebrand, Phys. Rev. 89, 1090-92, (1953).

APPENDIX

For a given photon energy the detection efficiency of the pair spectrometer is determined by the following items:

(1) Fraction of incident photons converted into pairs with a division of energy in the detectable interval.

(2) Fraction of pairs surviving against scattering and radiative collisions in the converter which would render them undetectable.

(3) Leakage of the particles between geiger tubes.

The evaluation of Item (1) is accomplished by integration of the differential pair production expression $\phi(W, \mu)$, as given by Rossi and Greisen[13], between the limits of the energy division parameter μ, for the pair energy W, which are allowed by the geometry. Figure 14 illustrates this process.

Due to a finite converter width, the average energy associated with a given pair of geiger tubes in this 90° spectrometer is slightly greater than that defined by considering all pairs to originate at the converter center. This is a 4 percent correction at the lowest energies, and 0.5 percent at the highest.

In the case of Item (2) the losses are kept small by the use of thin converters of small height. At a given magnetic field setting the scattering caused negligible spectrum distortion due to the cancellation of the effects of particle energy and solid angle upon scattering loss. Also the energy degradation effects due to radiative collisions in the thin converters (< 0.010 ins. Ta) produce negligible distortion for spectra of this breadth. However, in the absolute yield experiment these effects must be accounted for, since larger converter thicknesses were used.

For a pair particle produced in dx at depth x in the converter, the probability of remaining within the vertical angle subtended by the converter is determined from the gaussian projected scattering pattern calculated for the appropriate electron energy and converter depth. It is required that both pair particles thus survive, and the contributions from all depths are integrated to provide the survival factor for the converter. For a 0.020 in. Ta converter and 100 Mev photons the loss is 10 percent.

The considerations of radiative collision loss were the following. For a given photon energy the detectable pair contribution from dx at depth x in the converter is (for unit incident flux density):

$$dn = e^{-N\sigma_1 x} (N\sigma_2 dx) \left[e^{-N\sigma_3(t-x)} \right] \left[e^{-N\sigma_3'(t-x)} \right] ;$$

where σ_1 = total pair production cross section

σ_2 = cross section for producing pairs within the detectable energy division interval

σ_3 = cross section for radiative collision by positron with sufficient energy loss to remove it from detection

σ_3' = same for electron

When the energy division is symmetric, $\sigma_3 = \sigma_3'$.

By integrating over converter thickness (t), the total yield of detectable pairs is found to be:

$$n = \frac{\sigma_2}{2\sigma_3 - \sigma_1} \; e^{-N\sigma_1 t} \left[1 - e^{-N(2\sigma_3 - \sigma_1)t} \right].$$

Apart from such losses as discussed above, the "effective" converter thickness to produce a yield n is simply

$$t' = n / N \sigma_2.$$

This is the means of calculating the "effective" converter thickness used as abscissa in Figure 12.

FIGURE CAPTIONS

Fig. 1   Illustration of π^o-decay photon kinematics.

Fig. 2   Qualitative illustration of nature of total spectrum.

Fig. 3   Diagram to illustrate method for inferring angular distribution.

Fig. 4   Plan view of pair spectrometer.

Fig. 5   Photon spectra at various angles of view from carbon target bombarded by 340 Mev protons.

Fig. 6   Spectrum of total photon emission from carbon target bombarded by 340 Mev protons.

Fig. 7   Kinetic energy spectrum of neutral pion yield.

Fig. 8   Kinetic energy spectra for neutral pion emission at various angles in mean CM frame.

Fig. 9   Angular distributions in mean CM frame for neutral pions of various energies.

Fig. 10   Arrangement of absolute yield experiment.

Fig. 11   Spectrometer counts vs. effective converter thickness in the absolute yield experiment. (The unusual ordinate units are related to the beam monitoring system).

Fig. 12   Photon spectra at reduced proton energies for supplementary angles.

Fig. 13   Experimental points on neutral pion yield from carbon vs. proton energy. The smooth curve is from theoretical calculation mentioned in text.

Fig. 14   Diagram illustrating calculation of energy channel efficiencies for pair spectrometer.
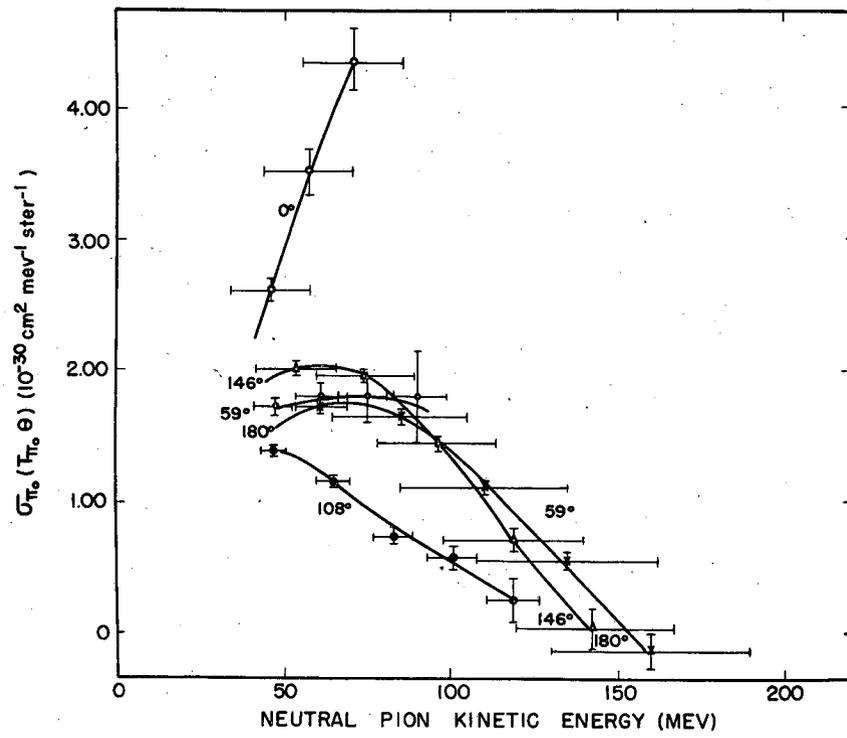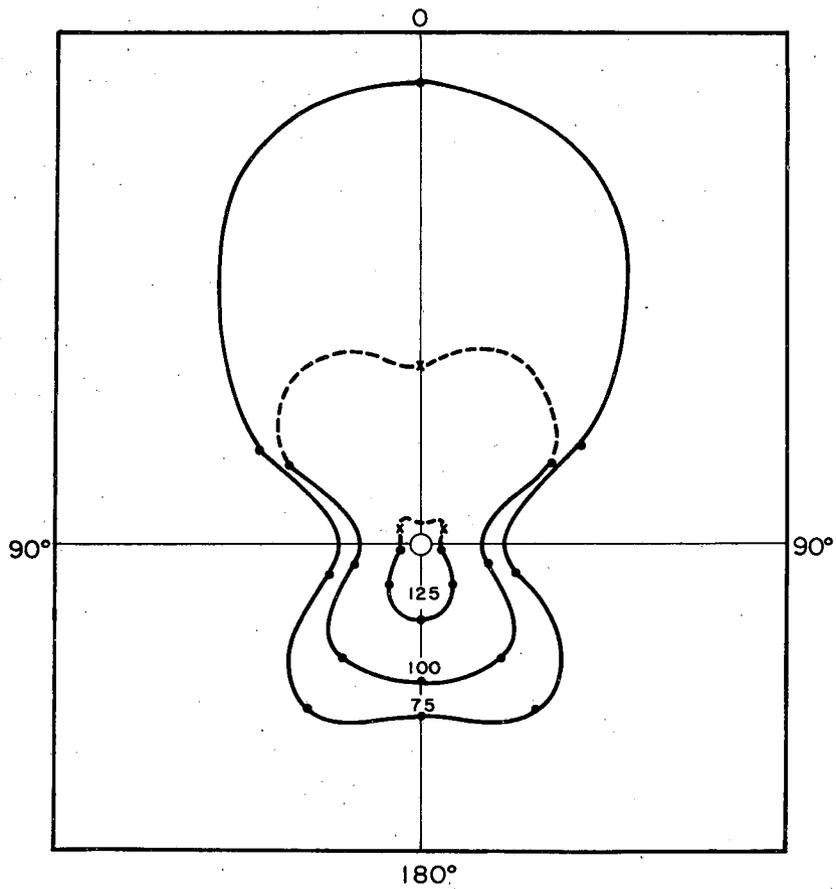
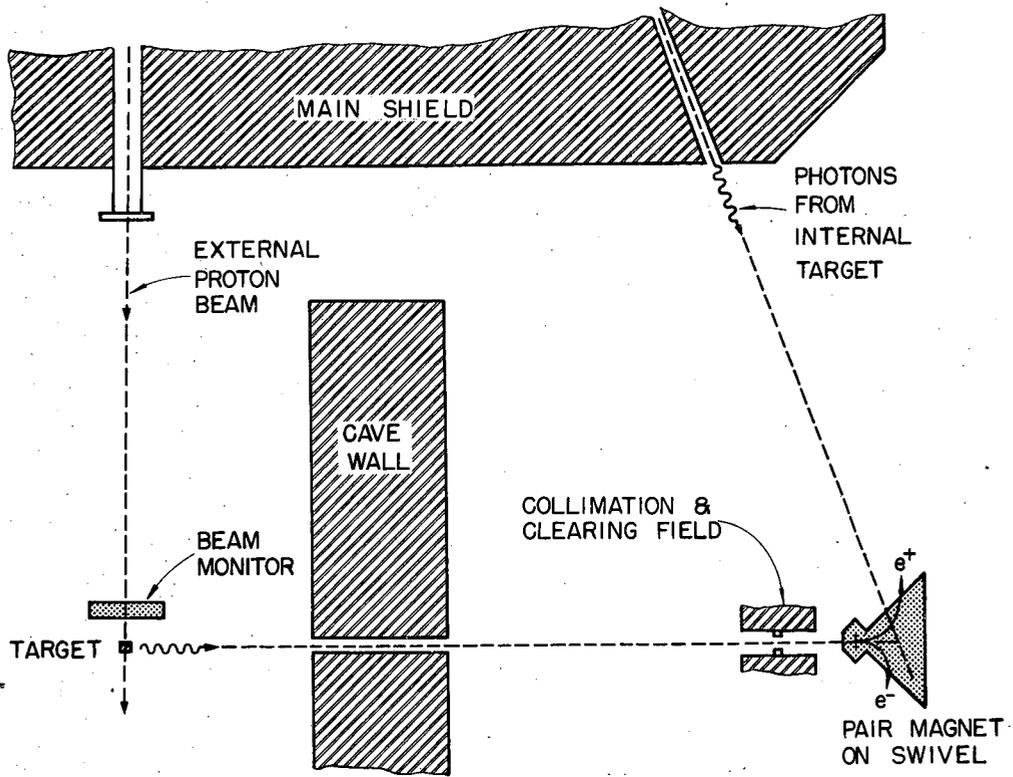MU-5159

Fig. 1

Fig. 2
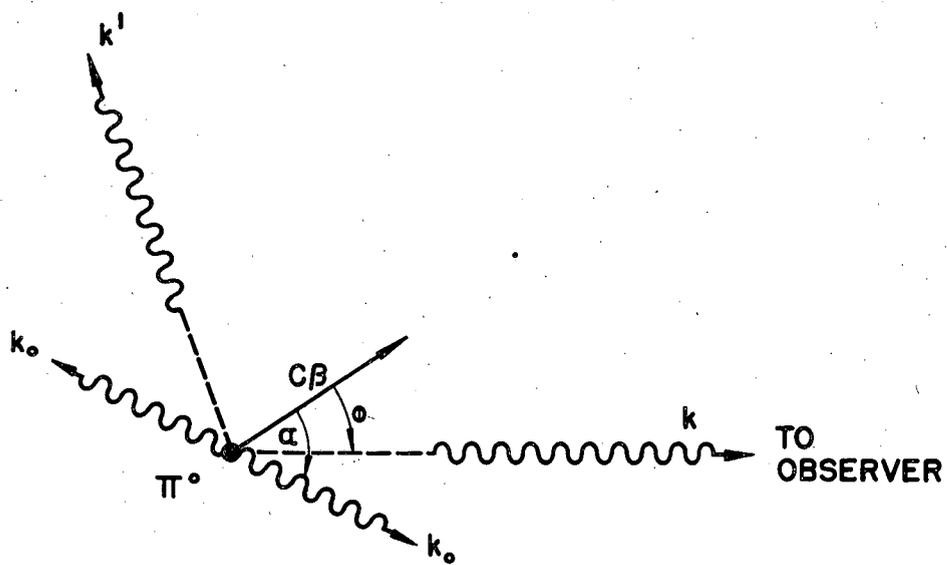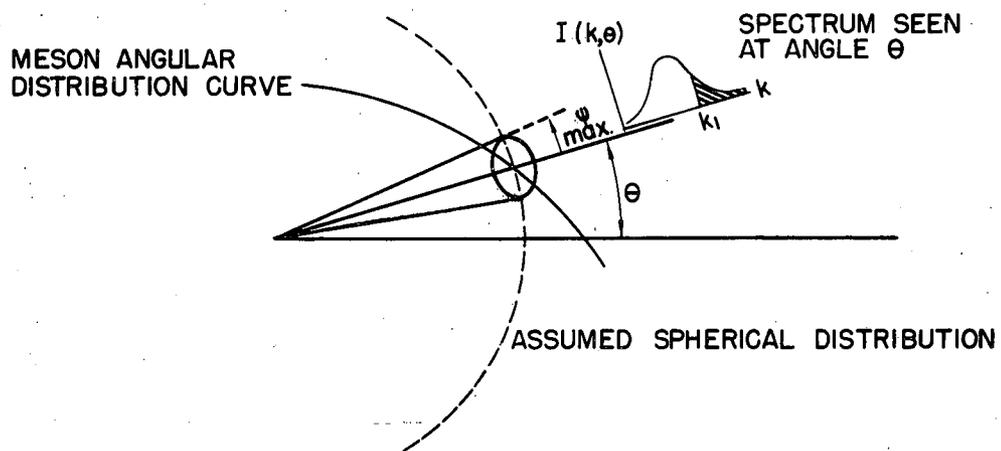
Fig. 3
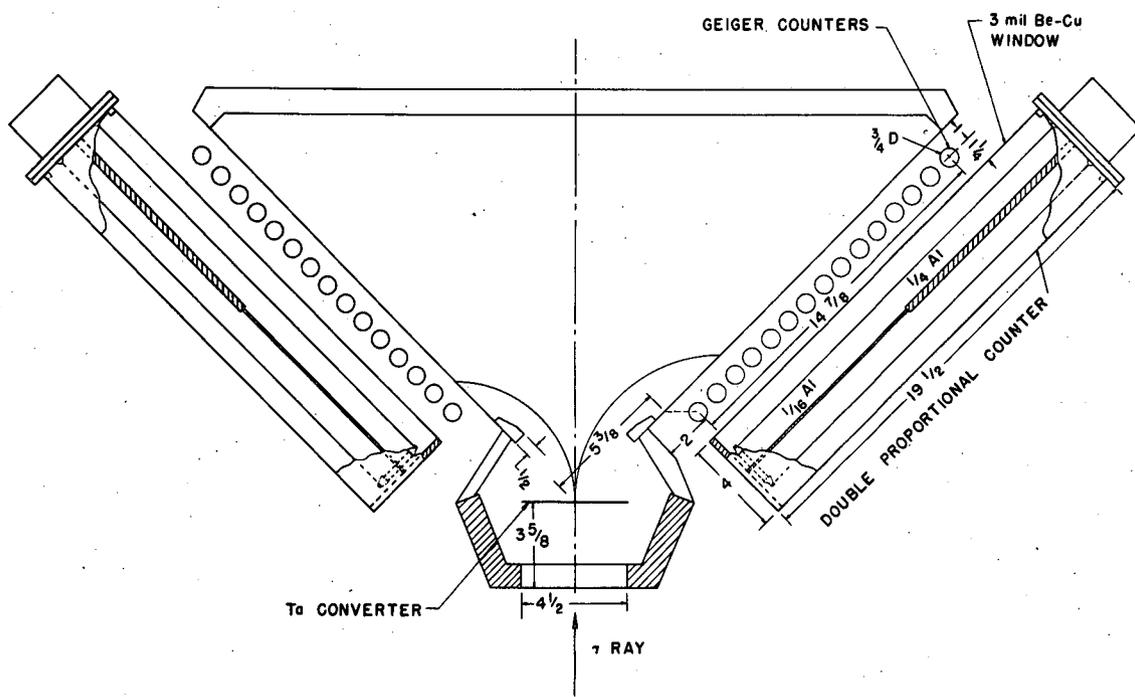
Fig. 4
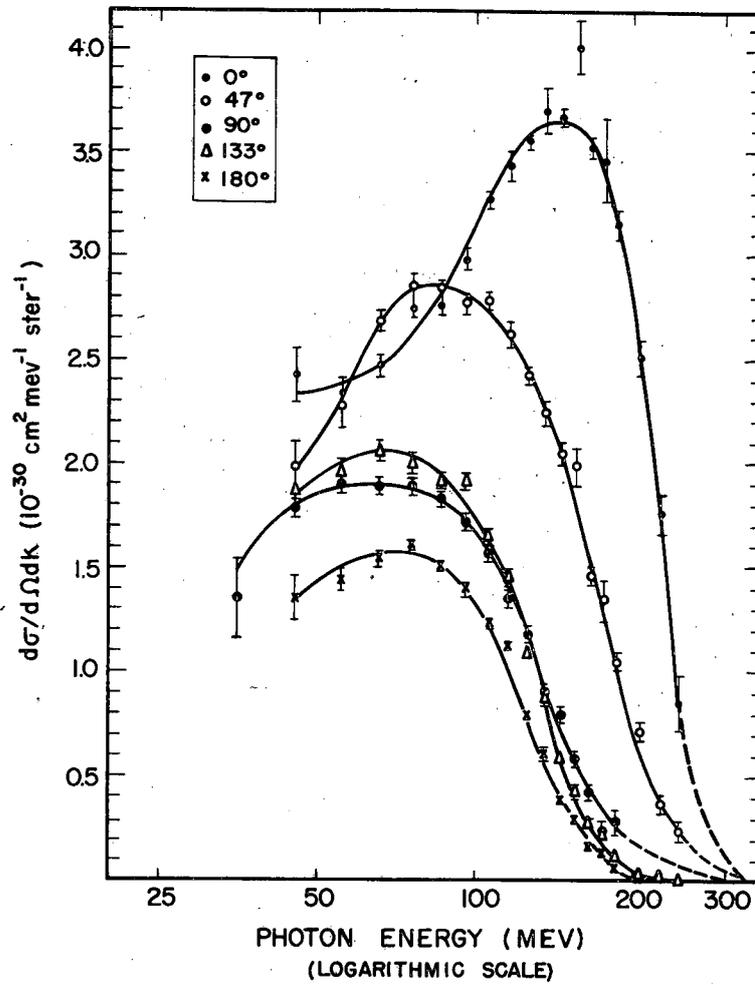
Fig. 5
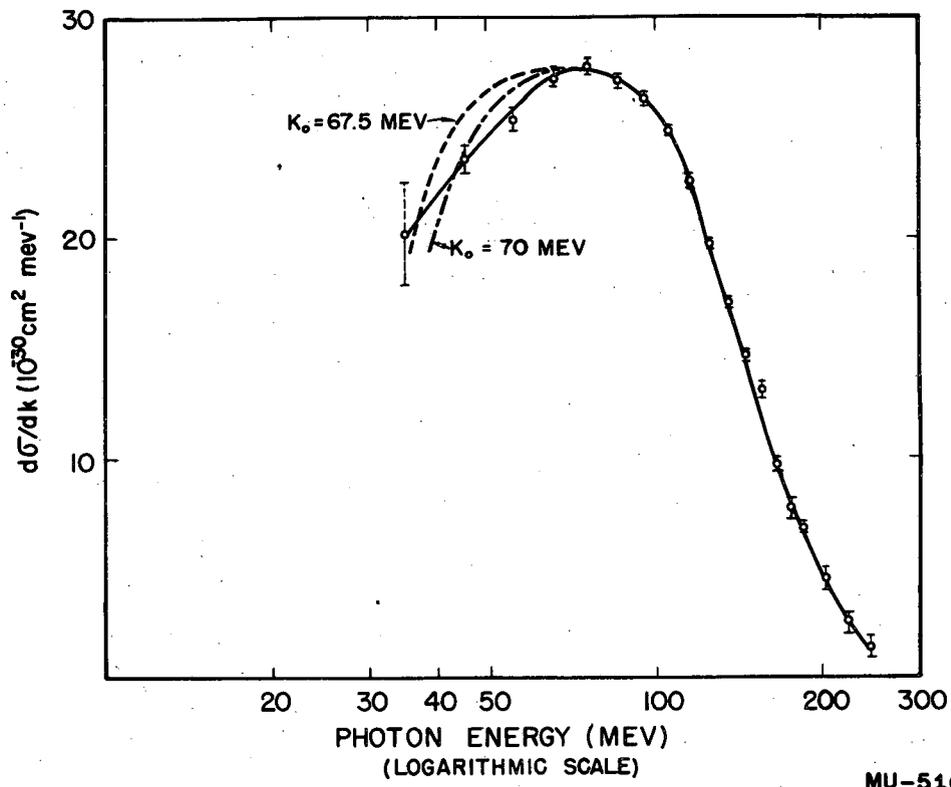
Fig. 6
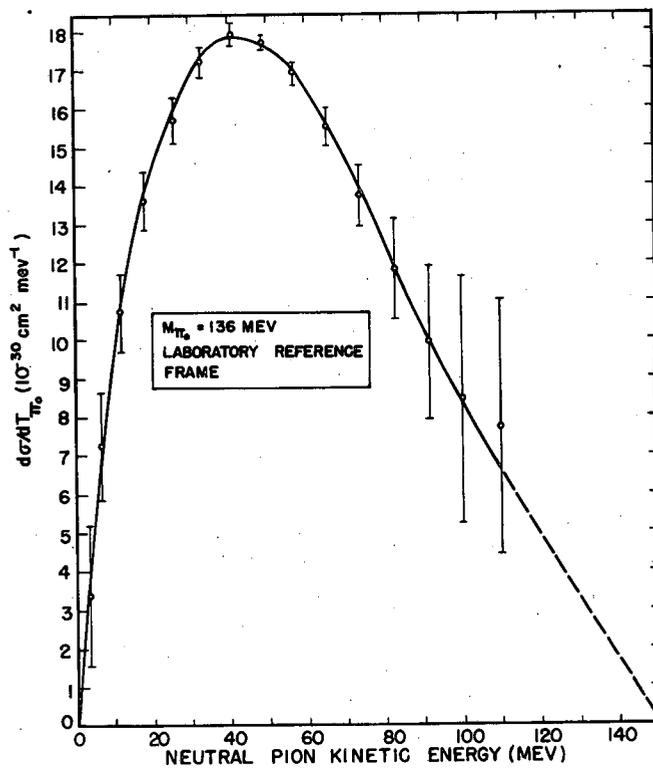
Fig. 7

MU-5164

MU-5165

Fig. 8
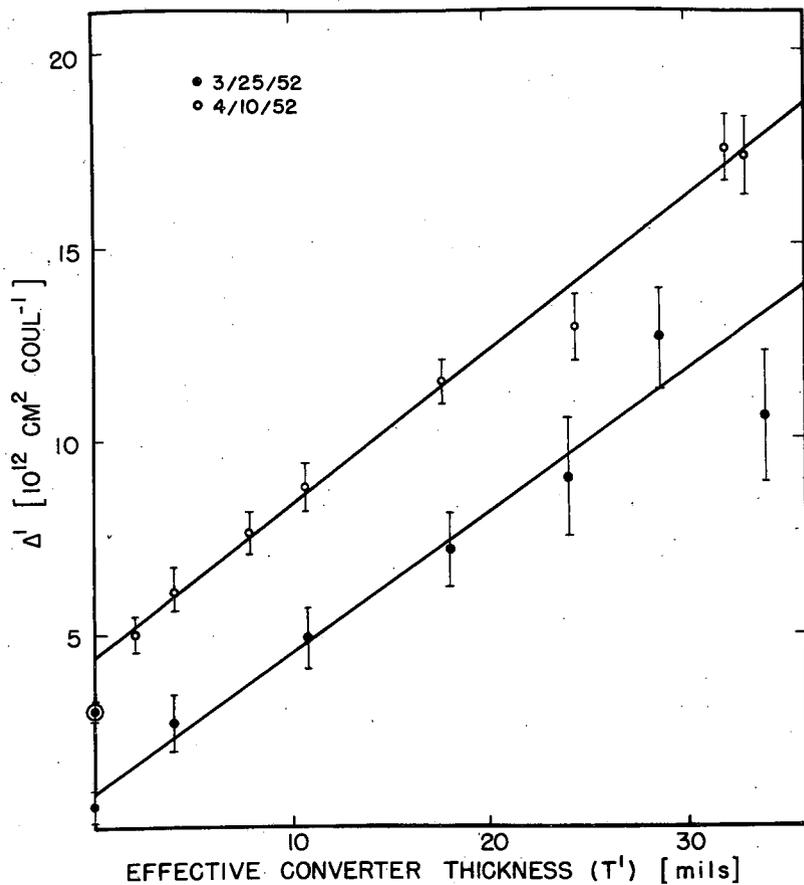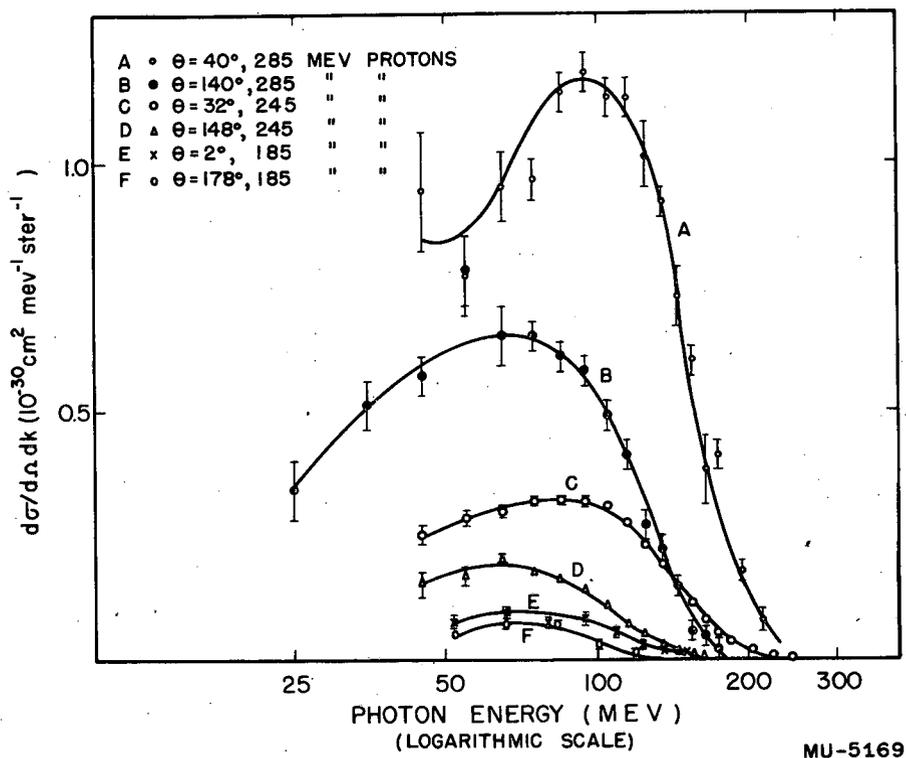
MU-5166

Fig. 9

Fig. 10

MU-5168

Fig. 11

Fig. 12

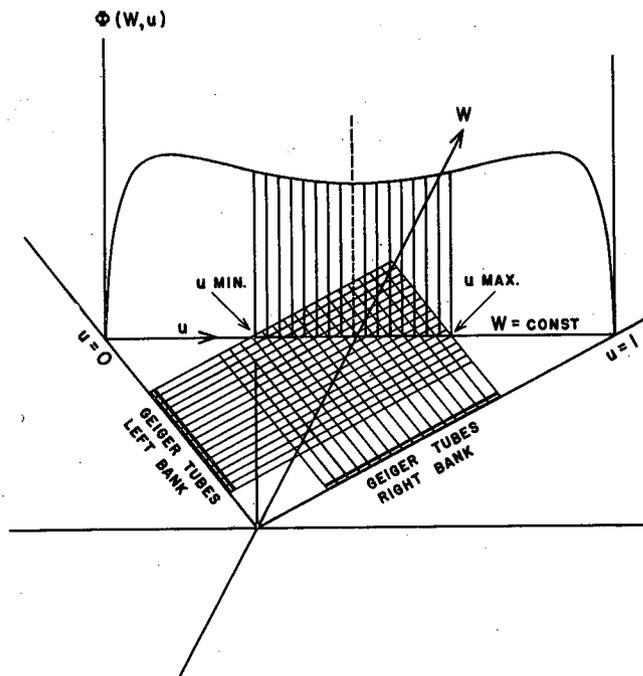Fig. 13

MU-5171

Fig. 14